JOURNAL OF MAGNETIC RESONANCE 60, 205–235 (1984)

Computer Simulations of Multiple-Quantum NMR Experiments. I. Nonselective Excitation

J. B. MURDOCH,* W. S. WARREN,† D. P. WEITEKAMP, AND A. PINES

Department of Chemistry and Materials and Molecular Research Division, Lawrence Berkeley Laboratory, University of California, Berkeley, California 94720

Received February 1, 1984

The multiple-quantum (MQ) evolution of anisotropic spin systems with four to eight coupled protons is analyzed using a computer for the basic three-pulse sequence. MQ intensities are first investigated as a function of preparation time. The concept of time-independent intensities is then introduced, and an algorithm for efficient computation of these quantities is described. A correlation between the distribution of dipolar coupling values and the intensity of high-quantum lines is discussed; in many cases, these intensities are predicted to be considerably larger than a simple statistical argument would suggest. The effect of varying the preparation and detection times independently is analyzed as a random walk problem.

INTRODUCTION

The conventional Fourier transform NMR experiment involves the creation and detection of single-quantum ($\Delta M = 1$) coherences. In recent years, however, multiple-quantum FT NMR (*1–8*) has opened new and uncharted regions of density matrix for exploration and development. Various groups have employed this new technique to study molecular conformation and motion (*9–11*), connectivities (*12*), relaxation (*13–18*), chemical shielding tensors (*2, 19*), and CIDNP (*20*). Additionally, MQ NMR has been used to analyze complicated isotropic spectra (*21–23*) and to overcome magnet inhomogeneity (*24*). Advantages include the ability to simplify complex spectra yet retain important structural information and the ability to isolate small, "interesting" parts of the Hamiltonian.

In this paper, we attack the problem of multiple-quantum intensities for coupled spin-1/2 systems. These intensities are of interest for several reasons. One is a practical consideration: can the higher-order transitions of use in the analysis of molecular structure and motion be excited with reasonable or at least detectable efficiency. A second reason is the importance of intensities in the determination of coupling constants and chemical shifts from experimental MQ spectra. An iterative least-squares fitting program (*25, 26*) can be used to generate multiple-quantum frequencies; calculation of the corresponding intensities can then confirm or throw doubt on the simulation. Finally, a third reason for studying MQ intensities is to

* Present address: Technicare Corporation, 29100 Aurora Rd., Solon, Ohio 44139.
† Present address: Department of Chemistry, Princeton University, Princeton, N.J. 08540.

0022-2364/84 $3.00

probe the relationship between exact quantum-mechanical dynamics and statistical behavior in multispin systems.

Our focus will be on molecules with four to eight protons dissolved in nematic liquid crystal solvents. For these multispin systems, a computer is necessary for calculation of the exact spin dynamics because matrices of interest range upward in size to 256 by 256 elements. The simplest three-pulse MQ experiment is analyzed here in detail. After some mathematical preliminaries and a look at zero-quantum selection rules, the growth of multiple-quantum coherence is studied as a function of preparation time τ and the value of ΔM. The effect of averaging spectra with different preparation times is considered, which leads to a calculation of τ-independent intensities. Finally, the effect of varying the preparation and detection times independently is investigated.

A subsequent paper (*27*) will extend this analysis to pulse sequences designed to selectively excite particular orders of multiple-quantum coherence.

BACKGROUND

Let us begin with the traditional flourish of Hamiltonians. For a system of N coupled spin-1/2 nuclei in an anisotropic medium, the Hamiltonian in the rotating frame comprises four terms (*28*):

$$\mathcal{H} = \mathcal{H}_D + \mathcal{H}_J + \mathcal{H}_{cs} + \mathcal{H}_{off} = \mathcal{H}_{internal} + \mathcal{H}_{off} \qquad [1a]$$

where

$$\mathcal{H}_D = \sum_{j<k}^{N} D_{jk}\left[I_{zj}I_{zk} - \frac{1}{2}(I_{xj}I_{xk} + I_{yj}I_{yk})\right] \quad \text{(direct dipolar couplings)} \qquad [1b]$$

$$\mathcal{H}_J = \sum_{j<k}^{N} J_{jk}\mathbf{I}_j \cdot \mathbf{I}_k \quad \text{(indirect } J\text{-couplings)} \qquad [1c]$$

$$\mathcal{H}_{cs} = \sum_{j}^{N} \sigma_j I_{zj} \quad \text{(relative chemical shifts)} \qquad [1d]$$

$$\mathcal{H}_{off} = -\Delta\omega I_z \quad \text{(overall offset frequency).} \qquad [1e]$$

The energy levels of $\mathcal{H}$ are divided into $N + 1$ manifolds, each corresponding to a different value of the Zeeman quantum number M and containing $N!/(N/2 + M)!(N/2 - M)!$ states. Splittings within all but the extreme Zeeman manifolds are due to the coupling and chemical-shift terms in $\mathcal{H}$. The number of possible transitions drops sharply as ΔM increases.

The simplest multiple-quantum pulse sequence contains three pulses (*3, 5, 19*) (Fig. 1a). Two pulses separated by a time τ are necessary to create multiple-quantum coherences, which then evolve for a time t_1. Because these coherences do not generate a rotating magnetization, they are not directly measurable. Hence a third pulse is needed to transform multiple-quantum coherence back to single-quantum coherence, which is detected after an additional delay t_2. One point is taken for

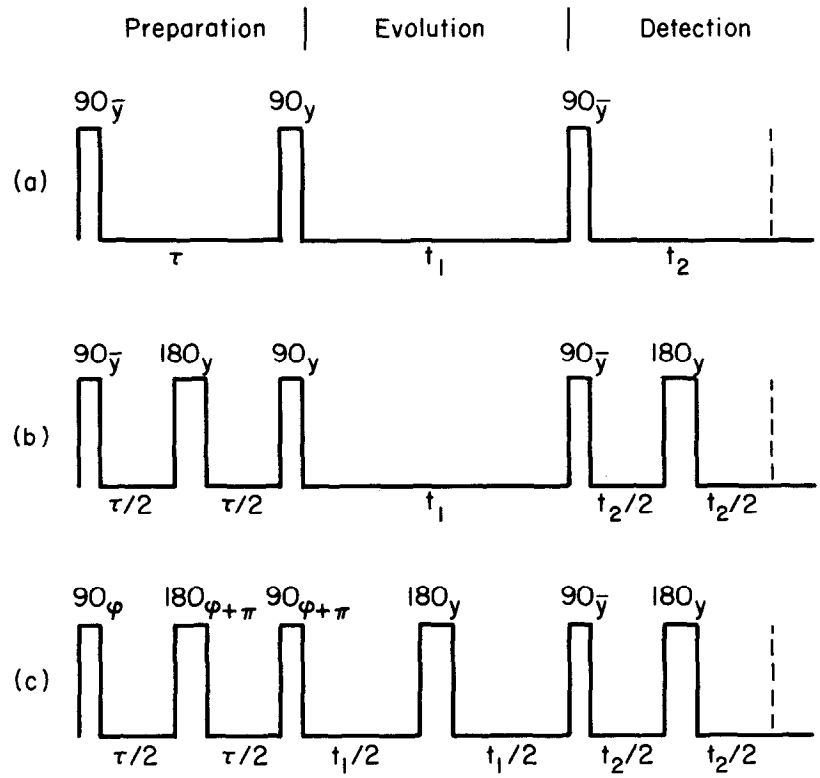

FIG. 1. (a) The simple three-pulse MQ sequence. (b) π pulses during the preparation and detection periods remove effects of the offset Hamiltonian, permitting even–odd selectivity for systems without chemical-shift differences. (c) In this TPPI sequence, the incrementation of preparation pulse phase as t_1 is increased separates different MQ orders. No rf frequency offset is then needed during evolution; hence a π pulse can be added to eliminate inhomogeneous line broadening.

each incremented value of t_1; the resulting MQ free induction decay is then Fourier transformed to yield the multiple-quantum spectrum. Different multiple-quantum orders (ΔM = 1, 2, 3, etc.) can be separated in this spectrum by an rf frequency offset (*2, 5*), by time-proportional incrementation of the preparation pulse phase (TPPI) (*6, 16*), by coherence transfer echoes (*29*), or by combining phase-shifted spectra (*4, 19*). The TPPI sequence is diagrammed in Fig. 1c.

A few assumptions will simplify the analysis of the three-pulse sequence. We will assume that $\|\mathscr{H}_{rf}\| \gg \|\mathscr{H}\|$, so that the internal Hamiltonian can be neglected during pulses. Each pulse can thereby be described in terms of a flip angle θ and an rf phase ϕ. We will deal almost exclusively with 90° flip angles. The first pulse will generally be chosen to be a $90\bar{y}$ pulse ($\phi = -90°$), rotating βI_z, the initial reduced equilibrium density matrix [$\beta = (\hbar\omega_0/kT)(2^{-N})$] to βI_x. Additionally, the rf detector in the rotating frame will be assumed to measure magnetization proportional to I_x. We will ignore relaxation effects since τ and t_2 are generally less than T_2 for the proton systems of interest. Finally, for simplicity we will assume a perfectly homogeneous magnetic field.

PROPERTIES OF THE PREPARED DENSITY MATRIX

Consider the preparation pulse sequence $90\bar{y}$–τ–$90y$ applied to an initial density matrix proportional to I_z. The propagator for this sequence is

$$U = \exp\left(i\frac{\pi}{2}I_y\right)\exp(-i\mathscr{H}\tau)\exp\left(-i\frac{\pi}{2}I_y\right) = \exp(-i\mathscr{H}_x\tau), \quad [2]$$

where $\mathscr{H}_x$ is a rotated Hamiltonian:

$$\mathscr{H}_x = \sum_{j<k}^{N} D_{jk}\left[I_{xj}I_{xk} - \frac{1}{2}(I_{yj}I_{yk} + I_{zj}I_{zk})\right] + \sum_{j<k}^{N} J_{jk}\mathbf{I}_j\cdot\mathbf{I}_k + \sum_{j}^{N}\sigma_j I_{xj} + \Delta\omega I_x \quad [3a]$$

$$\equiv \mathscr{H}_{xx} + \sum_j \sigma_j I_{xj} + \Delta\omega I_x. \quad [3b]$$

(Bilinear spin operators are lumped into $\mathscr{H}_{xx}$.) The prepared density matrix immediately following the sequence is given by

$$\beta P = U\beta I_z U^\dagger = e^{-i\mathscr{H}_x\tau}\beta I_z e^{i\mathscr{H}_x\tau}. \quad [4]$$

In general, $\mathscr{H}_x$ contains zero-quantum, one-quantum, and two-quantum operators, and the complex exponential can yield matrix elements of P corresponding to all multiple-quantum orders.

Consider now a system with no chemical shifts. If $\Delta\omega = 0$ (either by setting the rf frequency to the center of the spectrum or by adding a 180° pulse in the middle of the preparation period, as in Fig. 1b), then

$$\beta P = e^{-i\mathscr{H}_{xx}\tau}\beta I_z e^{i\mathscr{H}_{xx}\tau}. \quad [5]$$

The propagator contains only even-quantum matrix elements and hence only even-quantum coherences can be prepared (*19*). Similarly, the sequence $90x$–τ–$90y$ applied to βI_z (equivalent to a $90\bar{y}$–τ–$90y$ sequence applied to the single-quantum operator βI_y) prepares only odd-quantum coherence.

When $\Delta\omega \neq 0$, the prepared density matrix oscillates between even- and odd-quantum selectivity. Since $[\mathscr{H}_{xx}, I_x] = 0$, the propagator in Eq. [4] is separable and

$$\beta P = e^{-i\mathscr{H}_{xx}\tau}e^{-i\Delta\omega I_x\tau}\beta I_z e^{i\Delta\omega I_x\tau}e^{i\mathscr{H}_{xx}\tau} \quad [6a]$$

$$= \cos\Delta\omega\tau\, e^{-i\mathscr{H}_{xx}\tau}\beta I_z e^{i\mathscr{H}_{xx}\tau} - \sin\Delta\omega\tau\, e^{-i\mathscr{H}_{xx}\tau}\beta I_y e^{i\mathscr{H}_{xx}\tau}, \quad [6b]$$

where the first term in Eq. [6b] is even-selective and the second is odd-selective.

It is also of interest to investigate the effect of a spin-inversion operator on P. Define Π as $e^{-i\pi I_x}$, the propagator for a $180x$ pulse. I_x commutes with $\mathscr{H}_x$, so

$$\begin{aligned}\Pi^\dagger P\Pi &= e^{-i\mathscr{H}_x\tau}\Pi^\dagger I_z\Pi e^{i\mathscr{H}_x\tau}\\ &= e^{-i\mathscr{H}_x\tau}(-I_z)e^{i\mathscr{H}_x\tau}\\ &= -P. \end{aligned} \quad [7]$$

In terms of a single matrix element,

$$P_{jk} = \langle\psi_j|P|\psi_k\rangle = -\langle\psi_j|\Pi^\dagger P\Pi|\psi_k\rangle = -\langle\Pi\psi_j|P|\Pi\psi_k\rangle. \quad [8]$$

In certain cases, $|\Pi\psi_k\rangle$ will itself be an eigenstate $|\psi_{\bar{k}}\rangle$ of $\mathscr{H}$. Two such cases are as follows:

(1) When the internal Hamiltonian is purely bilinear ($\mathscr{H} = \mathscr{H}_D + \mathscr{H}_J$), it commutes with Π. For all ψ_k,

$$\mathscr{H}(\Pi\psi_k) = E_k(\Pi\psi_k). \qquad [9]$$

(2) For *any* Hamiltonian, the effect of Π on the lone $M = N/2$ eigenstate $|+ + + \cdots +\rangle$ is to flip all the spins, creating the lone $M = -N/2$ eigenstate $|- - - \cdots -\rangle$.

The frequency $\omega_{k\bar{k}}$ of a spin-inversion transition is independent of any bilinear term in the Hamiltonian (*8*). Thus in a system with no chemical-shift differences, each transition $|k\rangle$ to $|\bar{k}\rangle$ occurs with frequency $(M_k - M_{\bar{k}})\Delta\omega$, simply a multiple of the effective rf offset. For N spins, these spin-inversion transitions [also called class 1 coherences (*16*)] lie at the center of the $(N - 2n)$-quantum spectra ($n = 0, 1, 2 \cdots$) and provide no information on $\mathscr{H}_{\text{internal}}$. Moreover, in these systems the spectrum of each MQ order is symmetric about its center at $\Delta M\Delta\omega$, since $(\omega_{jk} - \Delta M\Delta\omega) = -(\omega_{\bar{k}\bar{j}} - \Delta M\Delta\omega)$.

A second property of spin-inversion transitions concerns the phase of the prepared density matrix element $P_{k\bar{k}}$ following a $90\bar{y}$–τ–$90y$ or $90x$–τ–$90y$ sequence. From Eq. [8], if spin-inversion pairs exist, then $P_{jk} = -P_{\bar{j}\bar{k}}$. In particular, for a spin-inversion transition $|k\rangle$ to $|\bar{k}\rangle$, $P_{k\bar{k}} = -P_{kk}$. Since P is Hermitian, $P_{k\bar{k}}$ must always be purely imaginary, no matter what the value of τ. In any system, therefore, statement (2) above implies that the highest quantum coherence is quantized along one axis of the complex plane, and its evolution is characterized by pure amplitude modulation (*3, 16*). In systems without chemical-shift differences, each eigenstate with $M \neq 0$ belongs to a spin-inversion pair, so the number of coherences restricted to one axis is

$$\frac{1}{2}[2^N] \qquad \text{for } N \text{ odd},$$

$$\frac{1}{2}\left[2^N - \binom{N}{N/2}\right] \qquad \text{for } N \text{ even}.$$

ZERO-QUANTUM SELECTION RULES

Spin-inversion properties give rise to additional selection rules for zero-quantum transitions between $M = 0$ states when N is even and $\mathscr{H}$ contains no chemical-shift differences. Then eigenstates of $\mathscr{H}$ and I_z can be chosen to be eigenstates of Π as well, with eigenvalues of $+1$ (*gerade*) or -1 (*ungerade*) (*30*). Since $\langle\psi_j|P|\psi_k\rangle = -\langle\Pi\psi_j|P|\Pi\psi_k\rangle$, transitions between $M = 0$ states with the same eigenvalue of Π are forbidden.

It should be stressed that these spin-inversion selection rules depend on the flip angle θ of the second preparation pulse. We have focused thus far on $\theta = 90°$. When $\theta = 45°$, however, it is possible in systems with no chemical-shift differences to select either the $g \leftrightarrow u$ or the $g \leftrightarrow g$, $u \leftrightarrow u$ $M = 0$ zero-quantum transitions merely by adjusting the rf phases.

Consider first the preparation pulse sequence $45x$–τ–$45\bar{x}$ applied on resonance to such systems. (The flip angle of the first pulse is set here at 45° to simplify the analysis; experimentally, a 90° pulse would be used to maximize the MQ signal.) The effective preparation Hamiltonian for this sequence is

$$\mathscr{H}_{45} = \exp\left(-i\frac{\pi}{4}I_x\right)\mathscr{H}\exp\left(i\frac{\pi}{4}I_x\right) \quad [10a]$$

$$= \frac{1}{2}\mathscr{H}_{xx} - \frac{3}{4}\sum_{j<k} D_{jk}(I_{yj}I_{zk} + I_{zj}I_{yk}) + \mathscr{H}_J. \quad [10b]$$

$\mathscr{H}_{45}$ commutes with Π; if

$$\beta P = e^{-i\mathscr{H}_{45}\tau}\beta I_z e^{i\mathscr{H}_{45}\tau}, \quad [11]$$

then $\Pi^\dagger P\Pi = -P$, as in Eq. [7].

In comparison, the pulse sequence $45\bar{y}$–τ–$45\bar{x}$ is equivalent to the previous x, $\bar{x}$ sequence acting on an initial density matrix proportional to I_x. In this case,

$$\beta P = e^{-i\mathscr{H}_{45}\tau}\beta I_x e^{i\mathscr{H}_{45}\tau} \quad [12]$$

and

$$\Pi^\dagger P\Pi = e^{-i\mathscr{H}_{45}\tau}\Pi^\dagger I_x \Pi e^{i\mathscr{H}_{45}\tau} = P. \quad [13]$$

Thus the first sequence prepares transitions between $M = 0$ states with different eigenvalues of Π, whereas the second sequence prepares transitions between $M = 0$ states with the same eigenvalue of Π. Note that because $\mathscr{H}_{45}$ contains both even-quantum and odd-quantum operators, neither sequence results in the even-odd selection described earlier for 90° pulses.

Figure 2 displays the *gerade-ungerade* selectivity in the zero-quantum spectrum of oriented benzene ($D_{12} = -817.1$ Hz). For the spectrum in Fig. 2a, the pulse sequence used was

$$90x\text{–}\frac{1}{2}\tau\text{–}180x\text{–}\frac{1}{2}\tau\text{–}45x\text{–}t_1\text{–}45x\text{–}\frac{1}{2}\tau\text{–}180x\text{–}\frac{1}{2}\tau,$$

where the π pulses simply remove any $\Delta\omega$ offset. For the spectrum in Fig. 2b, the $45x$ pulses were changed to $45y$ pulses. In each case, magnitude spectra corresponding to seven different values of τ between 4 and 16 ms were averaged together. The magnet homogeneity was sufficiently poor that only zero-quantum transitions appeared as sharp lines (*4*); hence, no special techniques were needed to separate MQ orders.

Lines present in both spectra are due to zero-quantum transitions between states with $M \neq 0$. Lines which appear solely in the first spectrum are due to $g \leftrightarrow u$ $M = 0$ transitions; the $g \leftrightarrow g$ and $u \leftrightarrow u$ transitions show up in the second spectrum. The simulations accompanying the experimental spectra are exact calculations for the actual values of τ that were used.

AN EXPRESSION FOR MULTIPLE-QUANTUM INTENSITY

Before discussing our computer results, we will first rewrite the prepared density matrix in a form more convenient for computation. The pulse sequence to be

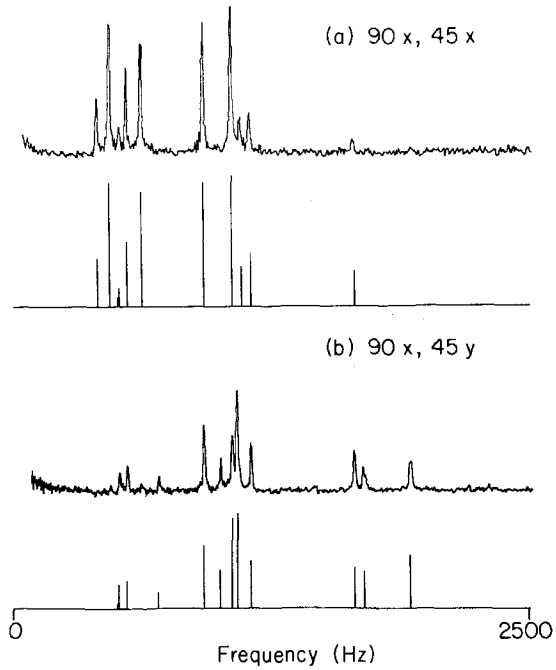

FIG. 2. *Gerade-ungerade* selectivity in the zero-quantum spectrum of oriented benzene. Each spectrum is an average over seven τ values from 4 to 16 ms, as are the accompanying simulations. (a) An on-resonance $90x$–τ–$45x$ preparation sequence excites $g \leftrightarrow u$ $M = 0$ transitions. (b) In contrast, an on-resonance $90x$–τ–$45y$ sequence prepares $g \leftrightarrow g$ and $u \leftrightarrow u$ transitions. Zero-quantum lines involving states with $M \neq 0$ appear in both spectra.

considered is $90\bar{y}$–τ–$90y$–t_1–$90\bar{y}$–t_2. The density matrix at the moment of detection may be written as

$$\rho(t_1; \tau, t_2) = e^{-i\mathscr{H}t_2}e^{-i(\pi/2)I_y}e^{-i\mathscr{H}t_1}e^{i(\pi/2)I_y}e^{-i\mathscr{H}\tau}\beta I_x e^{i\mathscr{H}\tau}e^{-i(\pi/2)I_y}e^{i\mathscr{H}t_1}e^{i(\pi/2)I_y}e^{i\mathscr{H}t_2}. \quad [14]$$

If R is the orthogonal transformation (or matrix of eigenvectors) which diagonalizes $\mathscr{H}$,

$$\mathscr{H} = RER^\dagger \qquad (E \text{ diagonal}), \quad [15]$$

we may define $X = R^\dagger I_x R$ as I_x expressed in the basis set of $\mathscr{H}$, and $A = R^\dagger \times \exp(-i(\pi/2)I_y)R$ as the pulse propagator in the basis set of $\mathscr{H}$. X and A are both real matrices and X is symmetric. With these definitions,

$$\rho(t_1; \tau, t_2) = \beta R e^{-iEt_2}Ae^{-iEt_1}A^\dagger e^{-iE\tau}Xe^{iE\tau}Ae^{iEt_1}A^\dagger e^{iEt_2}R^\dagger. \quad [16]$$

The signal $s(t_1; \tau, t_2)$ equals $\mathrm{Tr}\{\rho I_x\}$. Now introduce $P(\tau)$ as the prepared density matrix and $Q(t_2)$ as the "devolved detection matrix"—I_x taken backwards in time to the start of the detection period. We write both in the basis set of $\mathscr{H}$:

$$P = A^\dagger e^{-iE\tau}Xe^{iE\tau}A \quad [17a]$$

$$Q = A^\dagger e^{iEt_2}Xe^{-iEt_2}A. \quad [17b]$$

In terms of these matrices,

$$s(t_1; \tau, t_2) = \beta \operatorname{Tr}\{e^{-iEt_1} P e^{iEt_1} Q\} = \beta \sum_{j,k} P_{jk} Q_{kj} e^{i(E_k - E_j)t_1}. \quad [18]$$

Fourier transforming with respect to the evolution time t_1 yields the multiple-quantum spectrum:

$$S(\omega; \tau, t_2) = \beta \sum_{j,k} P_{jk} Q_{kj} \delta(\omega - \omega_{kj}). \quad [19]$$

The intensity of each multiple-quantum line is thus determined by the product of the two complex matrix elements, with

$$\begin{aligned} P_{jk} &= \sum_{a,b} A^{\dagger}_{ja} X_{ab} A_{bk} e^{i\omega_{ba}\tau} \\ &= \sum_{a,b} A_{aj} X_{ab} A_{bk} e^{i\omega_{ba}\tau} \\ &= \sum_{a,b} B_{ab} e^{i\omega_{ba}\tau} \end{aligned} \quad [20]$$

and

$$\begin{aligned} Q_{kj} &= \sum_{a,b} A^{\dagger}_{kb} X_{ba} A_{aj} e^{i\omega_{ba}t_2} \\ &= \sum_{a,b} A_{aj} X_{ab} A_{bk} e^{i\omega_{ba}t_2} \\ &= \sum_{a,b} B_{ab} e^{i\omega_{ba}t_2}. \end{aligned} \quad [21]$$

(B, a real matrix, is different for each transition $|j\rangle$ to $|k\rangle$. For convenience though, we will not include an explicit j, k label.) Because X is a single-quantum operator, $|M_a - M_b| = 1$ and the frequencies ω_{ba} correspond to symmetry-allowed single-quantum transitions. These dephase during the preparation period and rephase during the detection period.

When $\tau = t_2$, $P_{jk}(\tau) = Q_{kj}(t_2)$ and the intensity and phase of a transition $|j\rangle$ to $|k\rangle$ are given by

$$S_{jk} = \beta P_{jk}^2 = \beta \{\sum_{a,b} B_{ab} e^{i\omega_{ba}\tau}\}^2. \quad [22]$$

This quantity is in general a complex number (except for spin-inversion transitions, for which $S_{k\bar{k}}$ is always real and negative); thus the multiple-quantum spectrum contains lines with many different phases (Fig. 3a). In comparison, the intensity of a single-quantum transition in the usual FT experiment is βX_{jk}^2; barring experimental misadjustments, all lines have the same phase.

With a more complicated pulse sequence, it is possible, at least in theory, to generate a multiple-quantum spectrum with all lines in phase. If τ were made equal to $-t_2$ by some time-reversal sequence (*31*) applied during preparation, then P_{jk} would equal Q_{kj}^* and for all transitions $|j\rangle$ to $|k\rangle$,

$$S_{jk} = \beta |P_{jk}|^2. \quad [23]$$

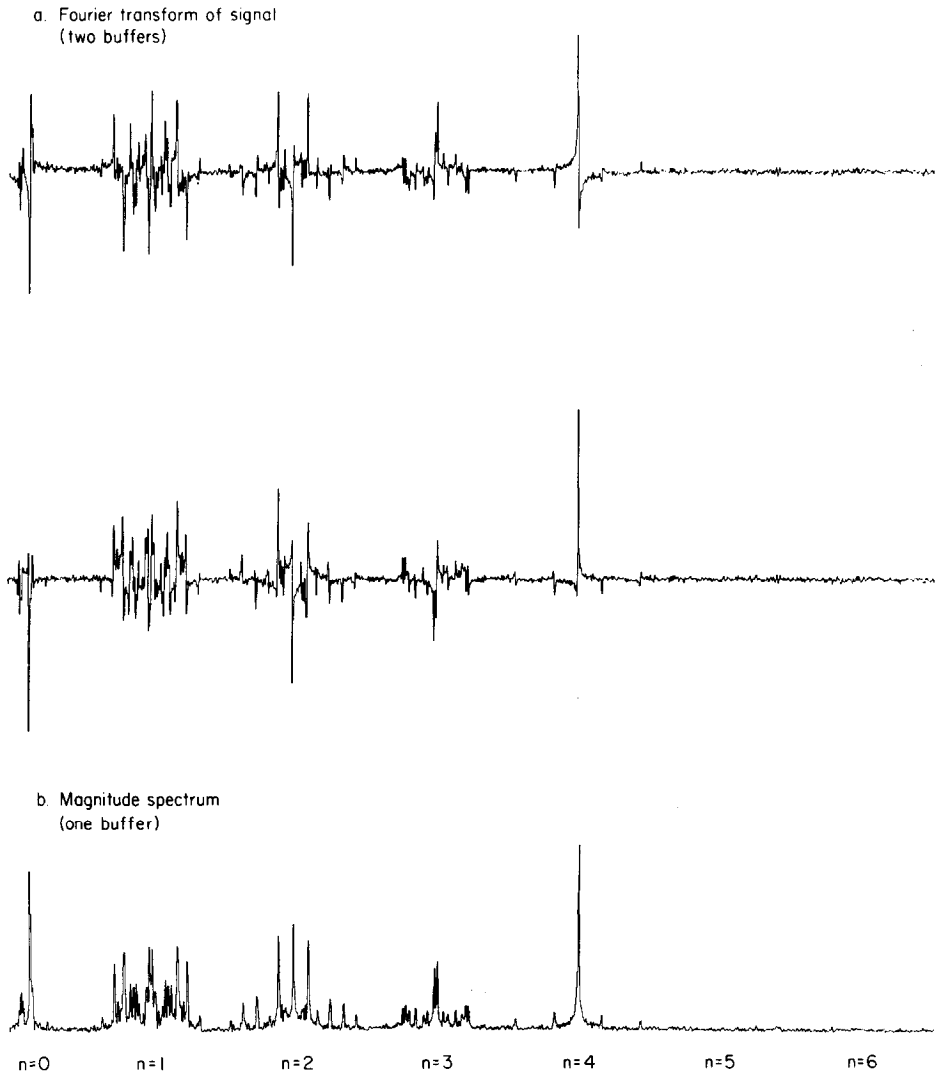

FIG. 3. The multiple-quantum spectrum of oriented benzene (14 wt% in Eastman nematic liquid crystal #15230) at 24.0° with $\tau = t_2 = 10$ ms and $\Delta\omega = 500$ Hz. The wide range of MQ phases apparent in (a) makes analysis difficult. The magnitude spectrum in (b) shows only slight broadening and is much more informative.

Time reversal (which may involve literally hundreds of pulses) is fortunately not necessary in many cases. Lines in the proton spectra of molecules dissolved in liquid crystals are narrow (3–10 Hz) in the absence of exchange and do not overlap in the interesting higher-quantum regions. A magnitude spectrum can therefore be calculated as in Fig. 3b (creating some line broadening due to dispersive tails) or each line can be phased individually. For $t_2 = \tau$, the resulting intensity of each transition $|j\rangle$ to $|k\rangle$ is again $\beta|P_{jk}|^2$. We therefore will focus on magnitude spectra obtained without time reversal. In solids, however, the existence of intermolecular

dipolar couplings gives rise to a continuum of transitions, and significant cancellation of intensity will occur if time-reversal sequences are not used (*32*).

COHERENCE MAGNITUDE AS A FUNCTION OF PREPARATION TIME

From Eq. [19] it is apparent that the intensities of multiple-quantum lines depend on the values of τ and t_2. For example, the calculated multiple-quantum magnitude spectra of oriented benzene for $\tau = t_2 = 0.25$, 5, and 100 ms are displayed in Fig. 4. Lines appear and disappear as the preparation and detection times are varied. To avoid missing a line due to an unfortunate choice of τ and t_2, magnitude spectra for different values of τ and t_2 can be averaged together, as in Fig. 5. Parameter-proportional phase incrementation (PPPI) (*33*) or comparable techniques (*34, 35*) can be used to quickly find an optimal set of τ values.

We have also computed, again for oriented benzene, the average prepared coherence magnitude $\beta|P_{jk}|$ for each multiple-quantum order as a function of τ. To

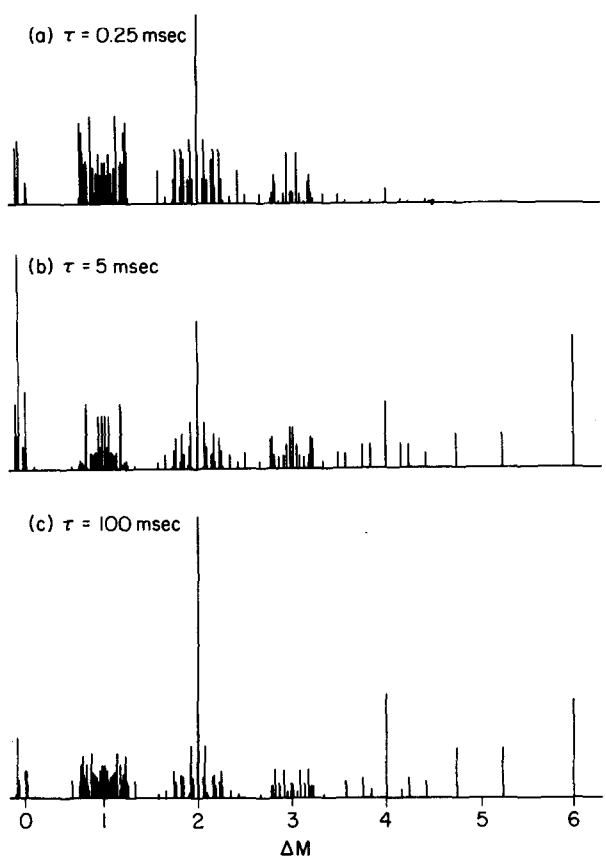

FIG. 4. Three calculated magnitude spectra for oriented benzene. The molecule was assumed to be hexagonal, with rapid reorientation about the C_6 axis. D_{12} was chosen to be −817.1 Hz, and isotropic J-coupling values were used. In the top spectrum, τ and t_2 are too short for higher-order transitions to be prepared or detected.

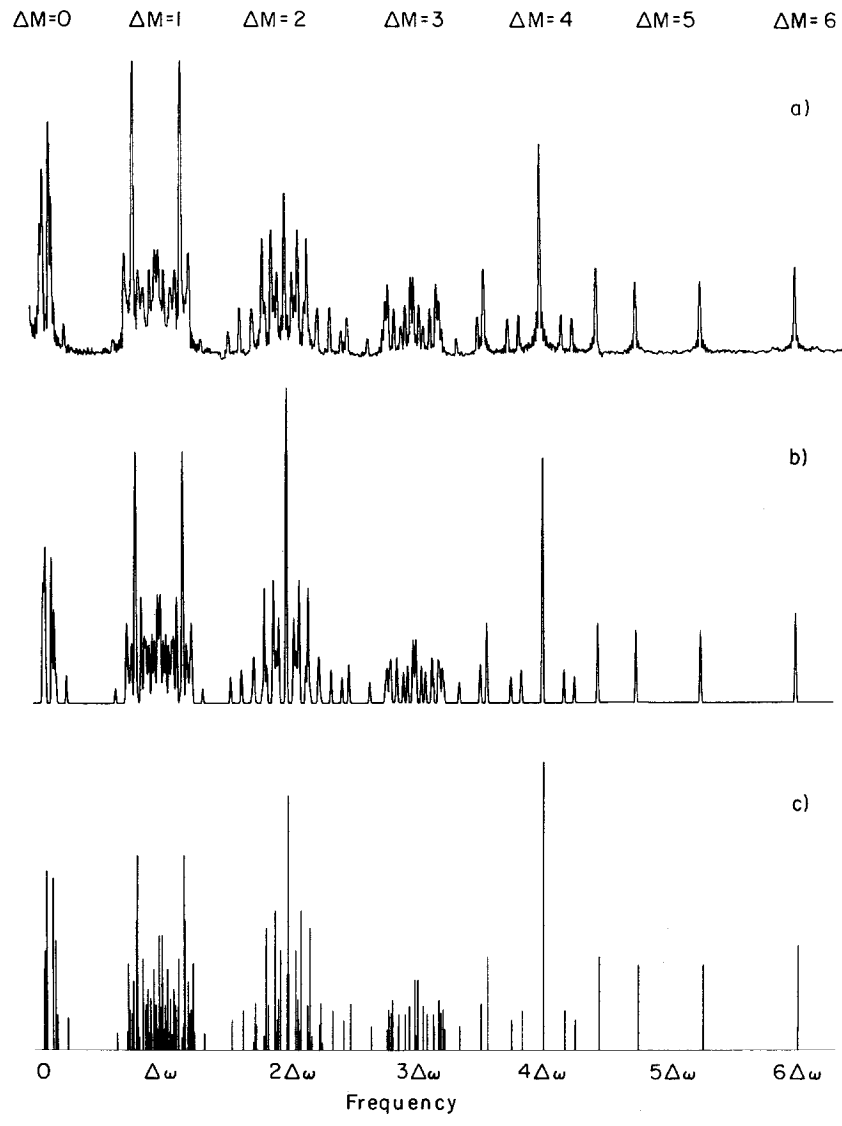

FIG. 5. The multiple-quantum spectrum of oriented benzene, averaged over four values of $\tau = t_2$ (4, 6, 8, and 10 ms). (a) Experiment, (b) simulation with broadening, (c) stick simulation. [Spectrum (a) reproduced, by permission of the publisher, from W. S. Warren, D. P. Weitekamp, and A. Pines, *J. Chem. Phys.* **73**, 2084 (1980).]

avoid even–odd selectivity, the two preparation pulses were chosen to differ in phase by 45°. Three such plots are displayed in Fig. 6. For the lower-quantum orders with many allowed transitions, the averaged coherence magnitude per transition is largely independent of τ after an initial "incubation" period [given roughly by $(2\pi\tau) \times$ (average dipolar coupling $\bar{D}$ in hertz) $\approx \pi/2$ or $\tau \approx (4\bar{D})^{-1} \approx 570$ μs in this case]. The single six-quantum coherence naturally shows greater oscillation but is also more intense on the average than a lower-order transition, as will be discussed later.

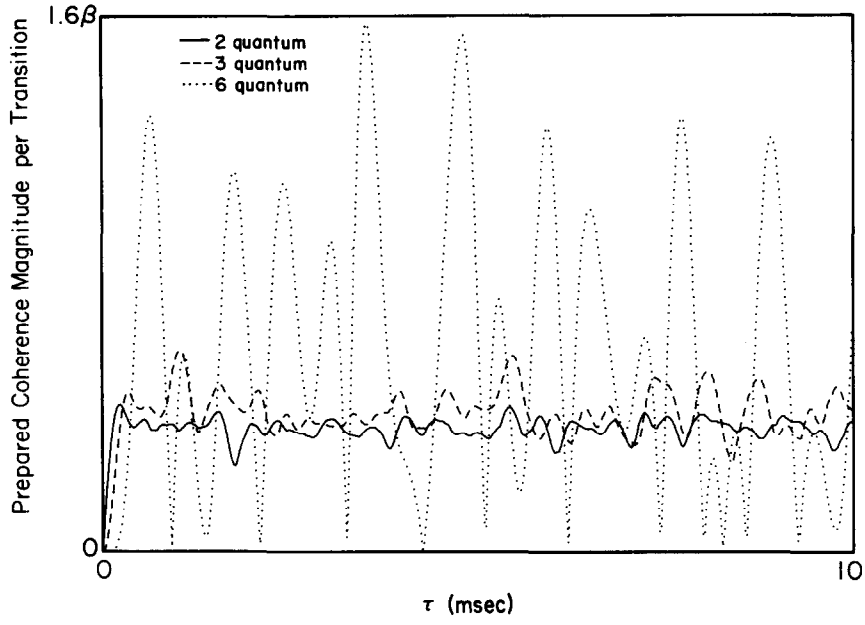

FIG. 6. Average prepared coherence magnitude $\beta|P_{jk}|$ as a function of τ for oriented benzene. The preparation sequence contained two $\pi/2$ pulses with a relative phase of 45°, and $\Delta\omega$ was assumed to be zero.

The normalized short τ behavior of prepared benzene coherence is presented in Fig. 7. (Again the two preparation pulses differ in phase by 45° to avoid even-odd selectivity.) For $\tau = 0$, only single-quantum coherence can be created; as τ increases, other orders of coherence appear. Higher-quantum transitions, in a sense more forbidden, require more time to be pumped. This dependence on τ can be quantified by expanding the prepared density matrix in a power series and evaluating commutators, as detailed in Ref. (*36*):

$$\beta P = e^{-i\mathscr{H}_x\tau}\rho_0 e^{i\mathscr{H}_x\tau}$$

$$= \rho_0 + i\tau[\rho_0, \mathscr{H}_x] - \frac{\tau^2}{2}[[\rho_0, \mathscr{H}_x], \mathscr{H}_x] + \cdots \qquad [24]$$

(ρ_0 can be βI_z or βI_x, depending on the phase of the preparation pulses.) Alternately, one can expand Eq. [20] and use the computer to calculate the $(P_{jk})_n$ terms:

$$P_{jk} = (P_{jk})_0 + i(P_{jk})_1\tau - \frac{1}{2}(P_{jk})_2\tau^2 + \cdots \qquad [25a]$$

$$(P_{jk})_n = \sum_{a,b} B_{ab}(\omega_{ba})^n. \qquad [25b]$$

The first nonzero commutator or $(P_{jk})_n$ term in the expansion determines the growth of coherence magnitude for short τ values. The exponents describing the τ power dependence of prepared coherence magnitude for different values of ΔM are listed

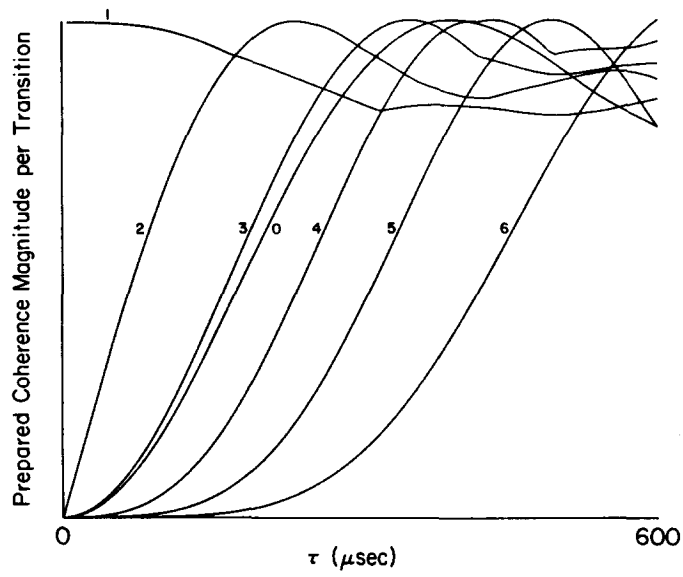

FIG. 7. Average prepared coherence magnitude at short values of τ for oriented benzene, with the same type of pulse sequence as in Fig. 6. The height of each curve has been normalized, and the τ power dependences calculated for the coherences match the values in the last column of Table 1. All orders of coherence are present when $2\pi|\bar{D}|\tau \approx \pi/2$ or $\tau \approx 570$ μs.

in Table 1. The τ power exponents for MQ spectral *intensity* in a $t_2 = \tau$ experiment would be double these numbers, since the effects of both preparation and detection must be included.

As an added feature of Table 1, the anisotropic spin systems we have been considering are compared with isotropic liquid systems. The fundamental difference between the two is the existence of nonscalar dipolar couplings in anisotropic systems. These couplings greatly facilitate the creation of multiple-quantum coherence; not only are they roughly 100 times larger than the *J*-couplings present in liquids, but their very form is such that lower powers of τ are sufficient to produce coherence (*36*).

STATISTICAL-LIMIT INTENSITIES

We turn now to the question of line intensities in the limit of a spectrum averaged over all possible values of τ. Such a spectrum should contain the "intrinsic" intensity for each line, free from the distortions due to a limited range of τ values.

The simplest estimate of τ-independent intensities is to assume that in the limit of long preparation times each symmetry-allowed coherence in the prepared density matrix will have the same magnitude but random phase. In this statistical limit, all symmetry-allowed transitions are excited equally (*19*). Figure 8a displays the statistical-limit multiple-quantum magnitude spectrum for benzene. Such spectra are easy to calculate but ignore the fact that some transitions are inherently stronger than others. In particular, these spectra often underestimate the intensity of higher-quantum lines, as will be discussed later.

TABLE 1

Dependence on τ of Multiple-Quantum Coherences Produced by the Sequence 90ϕ–τ–$90y$

		Initial τ power dependence		
	ΔM	$\phi = -90°$ [a]	$\phi = 0°$ [a]	$\phi = -45°$ [b]
Anisotropic systems	0	2	1	1 [c]
	1	1	0	0
	2	1	2	1
	3	3	2	2
	4	3	4	3
	n (even)	$n-1$	n	$n-1$
	n (odd)	n	$n-1$	$n-1$
Isotropic systems	0	2	1	1
	1	1	0	0
	2	3	4	3
	3	5	6	5
	4	7	8	7
	n (even)	$2n-1$	$2n$	$2n-1$
	n (odd)	$2n-1$	$2n$	$2n-1$

[a] For systems without chemical-shift differences, $\phi = -90°$ is even-selective and $\phi = 0°$ is odd-selective when $\Delta\omega = 0$.

[b] $\phi = -45°$ is equivalent to a superposition of $\phi = -90°$ and $\phi = 0°$ results.

[c] In systems without chemical-shift differences, only even-selective terms can prepare zero-quantum coherence. For these systems, the appearance of zero-quantum coherence is therefore proportional to τ^2.

For the $\tau = t_2$ MQ experiment, the total magnitude spectrum intensity plus the sum of the squares of the associated populations is given by

$$\beta \sum_{j,k} |P_{jk}^2| = \beta \, \mathrm{Tr}\{P^2\}. \qquad [26]$$

Since the trace is invariant to unitary transformations,

$$\mathrm{Tr}\{P^2\} = \mathrm{Tr}\{I_z^2\} = N2^{(N-2)}. \qquad [27]$$

The number of density matrix elements is 2^{2N} (coherences plus populations). The statistical-limit intensity per transition in multiples of β is thus $N2^{-(N+2)}$ and the statistical-limit value for coherence magnitude $|P_{jk}|$ is just the square root of this number.

The integrated spectral intensity per order is merely the intensity per transition times the number of allowed transitions. For nonsymmetric systems, the number of ΔM-quantum transitions is given by the following expressions (*13*):

$$\binom{2N}{N-\Delta M} \quad \text{for } \Delta M \neq 0,$$

$$\frac{1}{2}\left[\binom{2N}{N} - 2^N\right] \quad \text{for } \Delta M = 0,$$

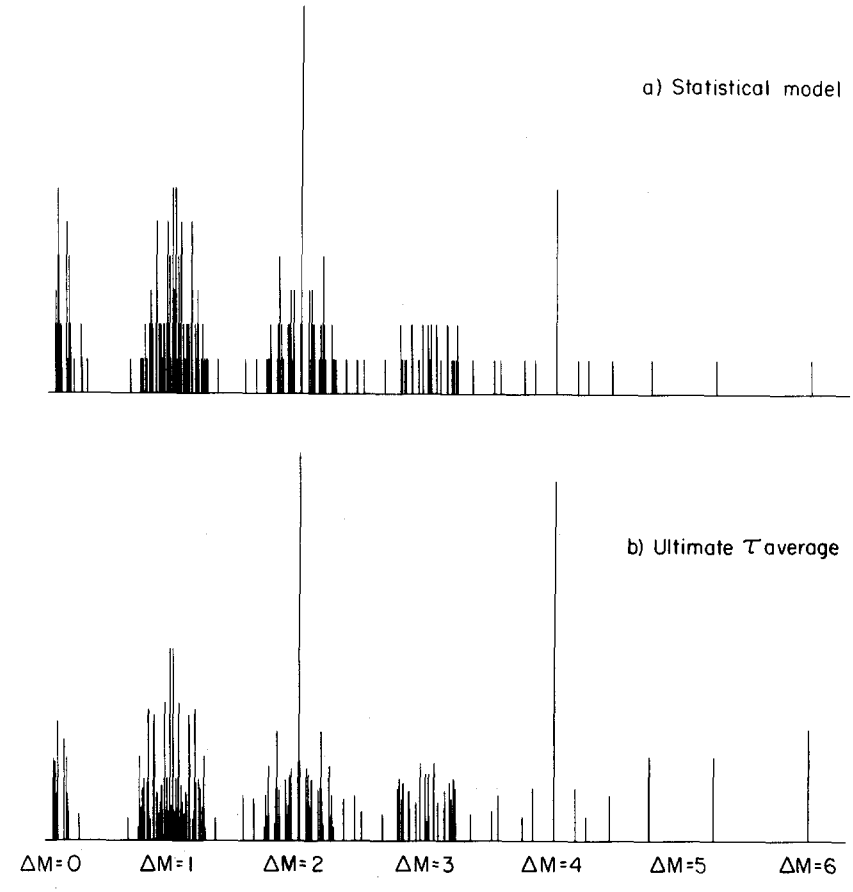

FIG. 8. Two τ-independent spectra calculated for oriented benzene. (a) The statistical-limit spectrum, in which every allowed transition is weighted equally. (b) The ultimate τ average spectrum.

or roughly

$$\frac{4^N}{\sqrt{N\pi}} e^{-(\Delta M)^2/N} \qquad \text{for } \Delta M \neq 0.$$

The integrated statistical-limit intensities per order in nonsymmetric four-, six-, and eight-spin systems are listed in Table 2. It can be seen that the statistical model suggests that simple nonselective excitation of high-quantum transitions will be very difficult to achieve.

For systems with symmetry, a more accurate approach is to calculate the statistical-limit intensity for each representation, equal to the initial magnetization β Tr(I_z^2) available to the representation divided by the number of elements in its reduced density matrix. This procedure is appropriate because each representation is in essence a separate system and evolves independently.

As an example, the A_1 representation of benzene contains thirteen states—one with $M = 3$, one with $M = 2$, three with $M = 1$, and three with $M = 0$, plus equivalent totals for $M < 0$. Hence

TABLE 2

Integrated Statistical-Limit Intensities vs Multiple-Quantum Order for Systems without Symmetry in Multiples of $\beta = (\hbar\omega_0/kT)(2^{-N})$

ΔM	8 spins	6 spins	4 spins
0	49.27	10.08	1.688
1	89.38	18.56	3.500
2	62.56	11.60	1.750
3	34.13	5.156	0.500
4	14.22	1.547	0.063
5	4.375	0.281	
6	0.938	0.023	
7	0.125		
8	0.008		

$$\mathrm{Tr}(I_z^2) = 2[1\cdot(3)^2 + 1\cdot(2)^2 + 3\cdot(1)^2] = 32, \qquad [28]$$

and the symmetry-adjusted intensity per A_1 transition is

$$\frac{32}{(13)^2}\beta = 0.189\beta, \qquad [29]$$

8.08 times the simple statistical-limit value of 0.0235β for a six-spin system.

In general, the number of symmetry-allowed coherences drops considerably when the overall density matrix is partitioned according to representation. As a result, the intensities of all remaining transitions are several times greater than the simple statistical-limit value of $\beta N 2^{-(N+2)}$. Different representations often have different average intensities, but for a given molecule these intensities vary by less than a factor of two or three. Hence, when plotted to the same height, the simple and symmetry-adjusted statistical-limit spectra for oriented benzene are comparable in appearance. The major difference is that the E-representation lines are smaller in the symmetry-adjusted spectrum, especially the E_2 lines.

ULTIMATE τ AVERAGE INTENSITIES

Another way to generate τ-independent intensities, for $t_2 = \tau$, is to actually average the τ-dependence contained in the expression for the magnitude of a given line. This "ultimate" τ average can be derived as follows. From Eq. [22],

$$\langle|S_{jk}|\rangle_\tau = \beta\langle|P_{jk}|^2\rangle_\tau = \beta\langle[\mathrm{Re}(P_{jk})]^2 + [\mathrm{Im}(P_{jk})]^2\rangle_\tau. \qquad [30]$$

Using Eq. [20],

$$\mathrm{Re}(P_{jk}) = \sum_{a,b} B_{ab}\cos\omega_{ba}\tau \qquad [31a]$$

and

$$\mathrm{Im}(P_{jk}) = \sum_{a,b} B_{ab}\sin\omega_{ba}\tau; \qquad [31b]$$

$$\langle |S_{jk}| \rangle_\tau = \beta \Big\langle \sum_{a,b} \sum_{a',b'} B_{ab} B_{a'b'} \cos(\omega_{ba} - \omega_{b'a'})\tau \Big\rangle_\tau$$

$$= \beta \sum_{a,b} B_{ab}^2 + \beta \sum_{a,b}{}' \sum_{a',b'}{}' B_{ab} B_{a'b'}, \qquad [32]$$

where the second set of summations is restricted: ω_{ba} must equal $\omega_{b'a'}$ and B_{ab}^2 terms are excluded.

Except for accidental degeneracies, there are only three circumstances for which single-quantum frequencies ω_{ba} and $\omega_{b'a'}$ would be expected to be equal. The first is the case of degenerate eigenstates in multidimensional irreducible representations, such as the doubly degenerate E_1 or E_2 states of benzene. Calculations indicate, however, that the sum over all $B_{ab}B_{a'b'}$ terms associated with the transitions between two sets of degenerate states is always zero.

The second cause for overlap of single-quantum frequencies is the existence of spin-inversion states. In this case $\omega_{\bar{b}\bar{a}} = \omega_{ba}$ and

$$\langle |S_{jk}| \rangle_\tau = \beta \sum_{a,b} B_{ab}^2 + \beta \sum_{a,b} B_{ab} B_{\bar{a}\bar{b}}. \qquad [33]$$

$B_{\bar{a}\bar{b}}$ can be shown to equal B_{ab} for ΔM even and $-B_{ab}$ for ΔM odd; hence

$$\text{for even-quantum transitions} \qquad \langle |S_{jk}| \rangle_\tau = 2\beta \sum_{a,b} B_{ab}^2, \qquad [34a]$$

$$\text{for odd-quantum transitions} \qquad \langle |S_{jk}| \rangle_\tau = 0. \qquad [34b]$$

This result is merely a manifestation of the even-quantum selectivity of the $90\bar{y}$–τ–$90y$ preparation sequence applied to systems with purely bilinear Hamiltonians. With the more general sequence

$$90\bar{y}\text{–}\tau\text{–}90\phi\text{–}t_1\text{–}90\bar{\phi}\text{–}\tau \qquad (\bar{\phi} = \pi + \phi),$$

the dependence of the ultimate τ average on the phase of the second and third pulses for these systems is as follows:

$$\text{for even-quantum transitions} \qquad \langle |S_{jk}| \rangle_\tau = 2\beta \cos^2 \phi \sum_{a,b} B_{ab}^2,$$

$$\text{for odd-quantum transitions} \qquad \langle |S_{jk}| \rangle_\tau = 2\beta \sin^2 \phi \sum_{a,b} B_{ab}^2. \qquad [35a]$$

To avoid the effect of even–odd selectivity when analyzing systems with no chemical-shift differences, we will choose $\phi = 45°$, for which simply

$$\langle |S_{jk}| \rangle_\tau = \beta \sum_{a,b} B_{ab}^2. \qquad [36]$$

The third cause for overlap of frequencies ω_{ab} and $\omega_{b'a'}$ is the extra single-quantum degeneracy in certain highly symmetric systems, such as D_2 or C_{4v} four-spin systems with $\bar{D} = 0$ or with no J couplings. Only for these special cases must the sum over $B_{ab}B_{a'b'}$ terms actually be calculated to obtain the correct intensity.

When the $B_{ab}B_{a'b'}$ terms can be ignored in Eq. [22], the computation of ultimate τ average intensities is greatly simplified. If we let $\mathcal{A}_{lm} = A_{lm}^2$ and $\mathcal{X}_{lm} = X_{lm}^2$, the

τ-averaged intensity of any transition $|j\rangle$ to $|k\rangle$ is given by a matrix element

$$\langle |S_{jk}| \rangle_\tau = \beta(\mathcal{A}^\dagger \mathcal{X} \mathcal{A})_{jk}. \quad [37]$$

This calculation requires no more multiplication than the calculation of S_{jk} for a single value of τ: roughly $2 \cdot 2^{2N} + 2 \cdot 2^{3N}$ real-number multiplications for a general N-spin system once A and X have been computed. {As a comparison, the use of Eq. [36] for every transition would entail $[(2^{2N} - 2^N)/2] \cdot [2 \cdot 2^{3N}]$ or approximately 2^{5N} multiplications.} The ultimate τ average spectrum for most systems can thus be generated much more quickly than an average over a number of discrete τ values.

Figure 8b displays the ultimate τ average spectrum of benzene. Although both this spectrum and the statistical-limit spectrum simulate the general features of the experimental results, the ultimate τ average approach more correctly predicts the intensity of individual lines. All transitions are not pumped equally; in particular, the lone six-quantum transition is appreciably stronger than an average isolated lower-quantum transition.

Figure 9 compares the experimental MQ spectrum of an eight-proton cyanobiphenyl liquid crystal (kindly supplied by Steven Sinton) with statistical-limit and ultimate τ average simulations. Of the two, clearly the ultimate τ average spectrum more accurately models such experimental features as the bimodality of the one-quantum region, the side peaks of the two-quantum region, and the enhanced intensity of the higher-quantum lines. That these latter transitions are in fact more intense than the ultimate τ average calculation would predict reflects a choice of experimental τ values fortuitous for the creation of high-quantum coherence.

Ideally, ultimate τ average intensities should match those obtained experimentally by averaging over a very large number of discrete τ values, but three possible problems with the ultimate method should be noted: (1) Overlapping transitions always add coherently as a sum of magnitudes rather than incoherently as a sum of complex values. (2) In the derivation of Eq. [32], it was assumed that each $\cos^2 \omega_{ba}\tau$ and $\sin^2 \omega_{ba}\tau$ term is averaged to 1/2, which will not be the case experimentally if $\omega_{ba}T_2^* \leqslant 1$. (3) The effect on intensities of a π pulse in the evolution period for a system with chemical shifts cannot be included. Nonetheless, these simulations can be used to quickly estimate the intrinsic strength of transitions and provide an efficient way of exploring intensity as a function of coupling and chemical shift parameters.

HIGHER QUANTUM SELECTIVITY IN THE ULTIMATE τ AVERAGE

It is worthwhile to study the ultimate τ average intensity per transition as a function of multiple-quantum order. Results for a number of molecules are listed in Table 3. In each case, the integrated intensity per MQ order decreases as ΔM increases, but the average intensity per transition is greater for larger ΔM. This increase in intensity per transition is most pronounced for systems possessing a high degree of symmetry or for systems whose dipolar couplings are similar in value, for which the quantity $d = \overline{D_{ij}}/(\overline{D_{ij}^2})^{1/2}$ is close to 1.0.

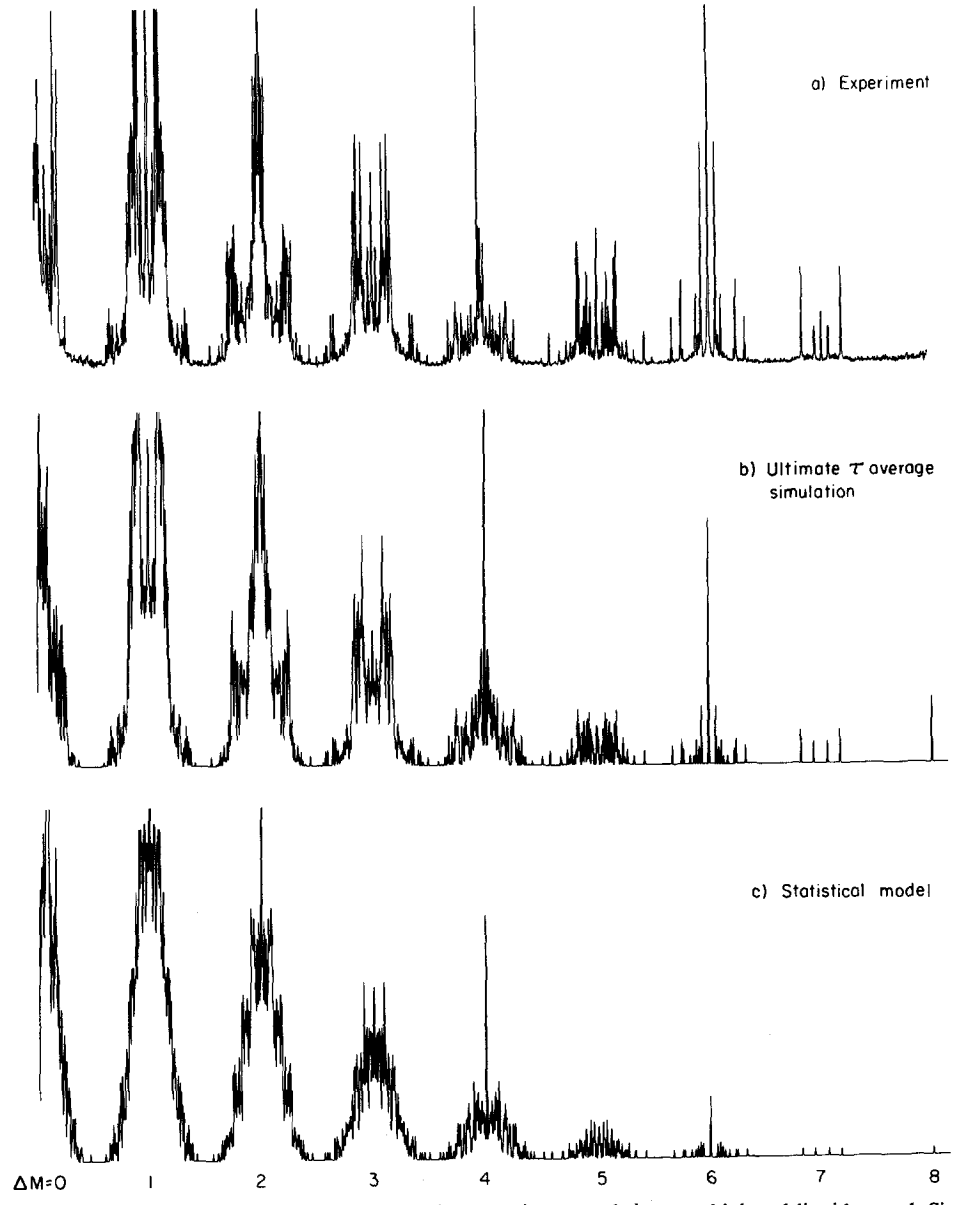

FIG. 9. (a) The proton TPPI MQ spectrum of a nematic *n*-pentyl-d_{11}-cyanobiphenyl liquid crystal. Six individual spectra with τ values ranging from 4 to 14 ms were averaged together. The eight-quantum line does not appear due to the choice of TPPI parameters, and the center line in the seven-quantum region is a TPPI artifact. (b and c) Two τ-independent simulations assuming D_4 spin symmetry. In all three spectra, the strongest zero-, one-, two-, and four-quantum lines have been clipped to better emphasize the overall lineshape. [Spectrum (a) reproduced, by permission of the publisher, from Ref. (*11*). The entire figure also appears in Ref. (*8*).]

To understand further the nature of this inherent high-quantum enhancement, consider the case of N magnetically fully equivalent spins in an anisotropic medium—an example would be the fluxional ten-spin molecule bullvalene dissolved

TABLE 3

Ultimate τ Average Intensity vs Multiple-Quantum Order for Various Molecules in Multiples of $\beta = (\hbar\omega_0/kT)(2^{-N})$

	Benzene	Cyclo-propane[a]	Cyclo-pentadiene[a]	2,5-Dichloro-acetophenone[a]	4,4'-Disubstituted biphenyl[b]	$CD_3(CH_2)_4CD_3$[c]
$D_{ij}/(D_{ij}^2)^{1/2}$:	0.777	0.567	0.028	0.225	0.519	0.080
			Integrated intensity			
$\Delta M = 0$	4.354	5.006	6.632	6.917	33.06	29.69
1	17.08	17.36	17.56	17.32	83.89	83.92
2	11.72	12.19	11.83	11.58	62.62	63.16
3	6.007	6.002	5.820	6.039	36.59	36.87
4	3.289	3.020	2.602	2.388	20.09	20.49
5	0.909	0.642	0.625	0.640	6.920	6.782
6	0.605	0.379	0.164	0.126	3.251	3.083
7					0.594	0.432
8					0.354	0.223
			Intensity per transition			
$\Delta M = 0$	0.109	0.132	0.060	0.051	0.029	0.020
1	0.147	0.152	0.072	0.060	0.038	0.029
2	0.148	0.158	0.073	0.063	0.040	0.031
3	0.177	0.177	0.075	0.069	0.043	0.034
4	0.274	0.252	0.093	0.075	0.053	0.043
5	0.455	0.321	0.104	0.080	0.060	0.048
6	0.605	0.379	0.164	0.126	0.108	0.086
7					0.148	0.108
8					0.354	0.223

[a] Coupling constants from Ref. (*28*).
[b] Coupling constants from Ref. (*11*).
[c] Coupling constants courtesy of G. Drobny, private communication, for the all-*trans* configuration.

in a liquid crystal (*37*). For such a system with unique dipolar coupling constant D and indirect spin–spin coupling constant J, $d = 1.0$ and

$$\mathscr{H} = \frac{3}{2} D \sum_{j<k}^{N} I_{zj} I_{zk} + \left(J - \frac{1}{2} D\right) \sum_{j<k}^{N} \mathbf{I}_j \cdot \mathbf{I}_k - \Delta\omega I_z.$$

The second term describes scalar coupling between equivalent spins and has no effect on the spectrum (*38*). The remaining terms commute with $\mathbf{I}^2$; hence the eigenstates can be separated into representations labeled by the value of $I(I + 1)$. As an example, the states of a four-spin system of this type divide into one quintet, three triplets, and two singlets (*39*). The number of allowed transitions is thus greatly reduced. In particular, there can be no zero-quantum transitions.

Line intensities can be calculated using the effective preparation Hamiltonian

$$\mathscr{H}_x = \frac{3}{2} D \sum_{j<k}^{N} I_{xj} I_{xk} - \Delta\omega I_x. \qquad [39]$$

The two terms of $\mathscr{H}_x$ commute, so

$$\beta P = \beta\left\{\exp\left(-i\frac{3}{2}D\tau\sum_{j<k}^{N} I_{xj}I_{xk}\right)\right\}(\cos\Delta\omega\tau\, I_z + \sin\Delta\omega\tau\, I_y) \times\left\{\exp\left(i\frac{3}{2}D\tau\sum_{j<k}^{N} I_{xj}I_{xk}\right)\right\}. \quad [40]$$

This expression can be evaluated using the relationships

$$\exp\left(-i\frac{3}{2}D\tau I_{xj}I_{xk}\right)I_{zj}\exp\left(i\frac{3}{2}D\tau I_{xj}I_{xk}\right) = \cos\left(\frac{3D\tau}{4}\right)I_{zj} - 2\sin\left(\frac{3D\tau}{4}\right)I_{yj}I_{xk} \quad [41a]$$

and

$$\exp\left(-i\frac{3}{2}D\tau I_{xj}I_{xk}\right)I_{yj}\exp\left(i\frac{3}{2}D\tau I_{xj}I_{xk}\right) = \cos\left(\frac{3D\tau}{4}\right)I_{yj} + 2\sin\left(\frac{3D\tau}{4}\right)I_{zj}I_{xk}. \quad [41b]$$

The prepared N-quantum coherence, given by the coefficient of $\prod_{i=1}^{N} I_{+i}$, is

$$\left(-\frac{i\beta N}{2}\right)(\cos\Delta\omega\tau)\left[\sin\left(\frac{3D\tau}{4}\right)\right]^{(N-1)} \quad \text{for } N \text{ even}, \quad [42a]$$

$$\left(\frac{i\beta N}{2}\right)(\sin\Delta\omega\tau)\left[\sin\left(\frac{3D\tau}{4}\right)\right]^{(N-1)} \quad \text{for } N \text{ odd}. \quad [42b]$$

The τ-averaged intensity for the N-quantum transition is

$$\beta N^2\left(\frac{1}{2}\right)^{2N+1}\frac{(2N-2)!}{(N-1)!(N-1)!}. \quad [43]$$

Table 4 presents these τ-averaged N-quantum intensities for several different values of N. Also included are computer-calculated values of τ-averaged integrated intensity

TABLE 4

Integrated Ultimate τ Average Intensities vs Multiple-Quantum Order for Equivalent-Spin Systems in Multiples of $\beta = (\hbar\omega_0/kT)(2^{-N})$

ΔM	8 spins	6 spins	4 spins
0	0	0	0
1	76.95	16.10	3.125
2	47.61	9.580	1.750
3	36.33	6.504	0.875
4	27.18	4.770	0.625
5	12.73	1.395	
6	10.21	1.107	
7	1.998		
8	1.676		

for lower multiple-quantum orders of these equivalent-spin systems. When $N = 8$, note that the integrated one-quantum and N-quantum intensities differ only by a factor of roughly 46; for a general eight-spin molecule, the difference would be a factor of 11,440 in the statistical limit.

Now return to the problem of a general N-spin system with arbitrary D_{ij}'s. Let $\bar{D}$ be the average value of the $N(N-1)/2$ dipolar couplings. The dipolar Hamiltonian can be written as

$$\mathscr{H}_D = \sum_{j<k}^{N} (D_{jk} - \bar{D})\left(\frac{3}{2} I_{zj} I_{zk} - \frac{1}{2} \mathbf{I}_j \cdot \mathbf{I}_k\right) + \bar{D} \sum_{j<k}^{N} \left(\frac{3}{2} I_{zj} I_{zk} - \frac{1}{2} \mathbf{I}_j \cdot \mathbf{I}_k\right), \qquad [44]$$

where the second term preferentially pumps higher quantum transitions. In going from a symmetric to a nonsymmetric system, this term will become less important and the integrated intensities of these higher quantum spectral regions will drop. However, the number of allowed lower quantum transitions increases rapidly as the symmetry is reduced, especially in the one- and two-quantum orders. Thus the τ-averaged intensity *per transition* is greater for large ΔM, even in completely general systems.

To illustrate this, we have calculated ultimate τ average intensities for nonsymmetric four-spin systems as a function of $\bar{D}$, the average value of the dipolar coupling. For each system, six dipolar couplings were generated randomly between ± 1000 Hz, and a constant value was added to each to fix the proper $\bar{D}$. Figure 10 displays the

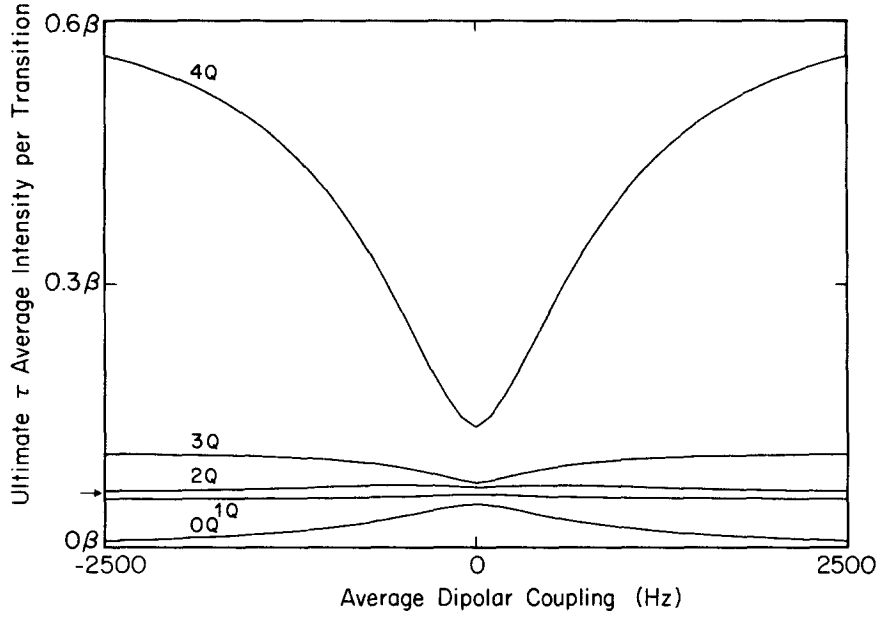

FIG. 10. Ultimate τ average intensity per transition for each MQ order as a function of the average dipolar coupling $\bar{D}$ in random four-spin systems. The arrow marks the statistical-limit intensity per transition (the same for all orders and all values of $\bar{D}$). Maximum range of D_{jk} values for each system: 2000 Hz.

resulting intensity per transition for each MQ order as the contribution of the average dipolar operator is varied. When $\bar{D}$ grows large compared to the range of dipolar couplings, the average four-quantum intensity naturally approaches its equivalent-spin value of 0.625β, or ten times the statistical-limit prediction. The average zero-quantum intensity drops toward zero. When $\bar{D}$ = 1000 Hz, yielding dipolar couplings in the range from 0 to 2000 Hz, the four-quantum line intensity is 6.5 times greater than the statistical-limit value.

Curiously enough, even when $\bar{D}$ equals zero, the four-quantum ultimate τ average intensity in Fig. 10 is still roughly twice as large as the statistical model would predict. This selectivity is due to other residual symmetry effects. For example, the τ-averaged four-quantum intensity of a hypothetical four-spin C_{3v} system with no chemical shifts or J couplings can be shown, after straightforward but lengthy evaluation of the appropriate matrices, to be given by the following formula (*40*):

$$\langle |S_{4Q}| \rangle_\tau (C_{3v}) = \frac{5}{64} \beta \frac{(29w^2 - 42vw + 45v^2)}{(7w^2 - 12vw + 9v^2)},$$

where $v = D_{12} = D_{13} = D_{23}$ and $w = D_{14} = D_{24} = D_{34}$. When $\bar{D} = 0$ ($v = -w$), the 4Q intensity is 0.324β, or 5.18 times the statistical value. Some of this selectivity carries over to general four-spin systems with $\bar{D} = 0$.

Even greater enhancement occurs when the number of spins increases. For $N = 6$, the ultimate τ average intensity of the six-quantum transition in a general system when $\bar{D}$ is comparable to the range of dipolar couplings is 27 times greater than the statistical-limit intensity per transition. The average five-quantum transition intensity is 3.9 times larger than the statistical value. For $N = 8$, the comparable enhancements are 150 and 13.

To summarize, nonselective excitation of high-quantum lines is, surprisingly, not so hopeless a procedure as the simple statistical-limit picture would imply, especially for systems with similar dipolar couplings. Even in completely general molecules, the residual selectivity of highly symmetric systems carries over and results in often sizeable improvement. This bodes well not only for ensemble-averaged MQ spectra but also for total spin coherence transfer echo experiments (*24*) and for symmetry selective NMR (*35, 41*).

AVERAGE INTENSITIES IN ISOTROPIC SYSTEMS

Ultimate τ average intensities in isotropic systems have also been briefly investigated. Here $\mathscr{H}_D = 0$ and thus J couplings are the sole source of spin–spin interaction. If multiple-quantum coherence is to develop, there must be chemical-shift differences as well; otherwise only single-quantum transitions can be prepared. (This can be seen by rewriting Eq. [6b] with $\mathscr{H}_{xx}$ equal to $\mathscr{H}_J$:

$$\beta \mathrm{P} = \cos \Delta\omega\tau e^{-i\mathscr{H}_J\tau} \beta I_z e^{i\mathscr{H}_J\tau} - \sin \Delta\omega\tau e^{-i\mathscr{H}_J\tau} \beta I_y e^{i\mathscr{H}_J\tau} \quad [46a]$$

$$= \cos \Delta\omega\tau \beta I_z - \sin \Delta\omega\tau \beta I_y \quad [46b]$$

since $[\mathscr{H}_J, I_z] = [\mathscr{H}_J, I_y] = 0$.)

The degree of higher-quantum excitation depends on the relative sizes of the J-coupling constants and the chemical-shift differences. In the first-order limit

($|\sigma_j - \sigma_k| \gg J_{jk}$), the N-quantum coherence magnitude can be shown (*36*) to be given by the following:

$$\frac{1}{2}\beta \sum_j \cos(\Delta\omega - \sigma_j)\tau \prod_{k\neq j} \sin(J_{jk}\tau/2) \qquad \text{for } N \text{ even,} \qquad [47a]$$

$$\frac{1}{2}\beta \sum_j \sin(\Delta\omega - \sigma_j)\tau \prod_{k\neq j} \sin(J_{jk}\tau/2) \qquad \text{for } N \text{ odd.} \qquad [47b]$$

(Eq. [47a] reduces to the formula in Ref. (*42*) for two-quantum coherence in an AX system.) The τ-averaged N-quantum intensity calculated from these expressions is exactly the statistical-limit value. Note, however, that for N-quantum coherence to develop after a reasonably short time τ, there must be at least one spin j with healthy couplings J_{jk} to all other spins. (This "cluster coupling" condition is not necessary for the creation of N-quantum coherence in anisotropic dipolar-coupled systems.) As for lower-quantum lines, computer simulation of first-order systems has shown that all transitions are on the average excited equally, in complete accord with the statistical model.

In contrast, for the strong-coupling limit ($J_{jk} > |\sigma_j - \sigma_k|$), the same sort of higher-quantum enhancement occurs as in anisotropic systems. Again the effect is most pronounced when the bilinear coupling constants (here the J_{jk} values) are nearly equal.

TOTAL SPECTRAL INTENSITY WHEN τ DOES NOT EQUAL t_2

Thus far, only the case of $t_2 = \tau$ has been considered. We will now examine the effect on signal intensity of varying τ and t_2 independently. Figure 11 is a calculation of the total intensity of the magnitude MQ spectrum of oriented benzene as a function of t_2 for two different values of τ. Figure 12 displays the total magnitude spectrum intensity for benzene over a range of τ and t_2 values. Clearly, there is something special, but not spectacular, about $t_2 = \tau$. A simple argument follows to explain why there is a maximum in total spectral intensity there and why this maximum is about 1.27 times the $t_2 \neq \tau$ "baseline."

Recall from Eq. [19] that the magnitude of a given MQ line can be written as

$$|S_{jk}| = \beta|P_{jk}(\tau)Q_{kj}(t_2)|. \qquad [48]$$

The ratio ξ of the total intensity at $t_2 = \tau$ relative to the "baseline" is

$$\xi = \frac{\sum_{j,k} |P_{jk}^2(\tau)|}{\left\langle \sum_{j,k} |P_{jk}(\tau)Q_{kj}(t_2)| \right\rangle_{t_2}}. \qquad [49]$$

Both numerator and denominator involve the summation of many transition intensities for one value of τ. We will assume that the same ratio holds if we look at a single MQ transition but average over many values of τ, in a sense substituting a time average for an ensemble average. That is, we assert that

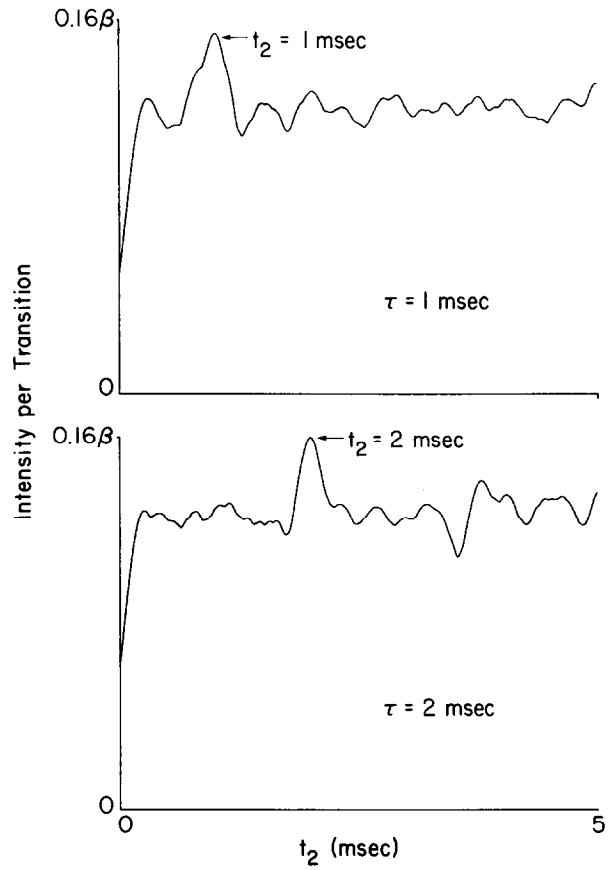

FIG. 11. Total magnitude spectrum intensity as a function of t_2 for oriented benzene, divided by the number of allowed transitions. In each plot there is a bulge when $t_2 = \tau$.

$$\xi \approx \frac{\langle |P_{jk}^2(\tau)| \rangle_\tau}{\langle \langle |P_{jk}(\tau) Q_{kj}(t_2)| \rangle_{t_2} \rangle_\tau} \qquad [50]$$

and concentrate on just a single line. $\langle |P_{jk}^2| \rangle_\tau$ is just the ultimate τ average intensity of the transition:

$$\langle |P_{jk}^2| \rangle_\tau = \sum_{a,b} B_{ab}^2. \qquad [51]$$

On the other hand,

$$\langle \langle |P_{jk}(\tau) Q_{kj}(t_2)| \rangle_{t_2} \rangle_\tau = \langle |P_{jk}| \rangle_\tau \langle |Q_{kj}| \rangle_{t_2}$$

$$= \langle |P_{jk}| \rangle_\tau^2 \qquad [52]$$

and hence

$$\xi = \langle |P_{jk}|^2 \rangle_\tau / \langle |P_{jk}| \rangle_\tau^2 \qquad [53a]$$

$$= \bar{\sigma}_{jk}^2 + 1, \qquad [53b]$$

where $\bar{\sigma}_{jk}$ is the relative standard deviation of $|P_{jk}|$.

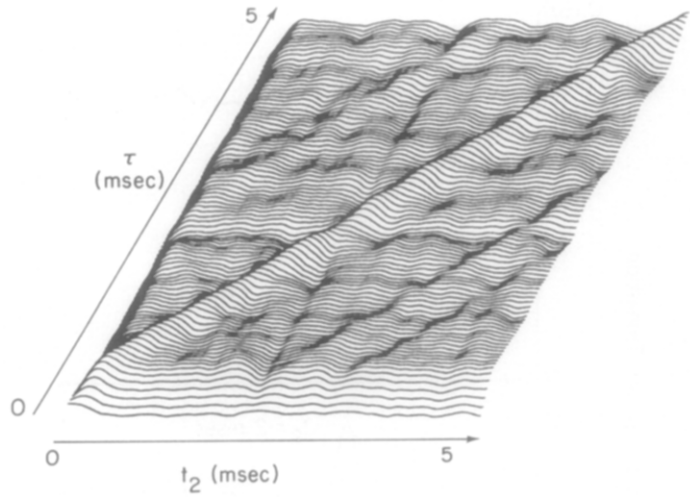

FIG. 12. Total magnitude spectrum intensity as a function of both τ and t_2 for oriented benzene.

For simplicity, rewrite P_{jk} as

$$P_{jk} = \sum_{a,b} B_{ab} e^{i\omega_{ba}\tau} \equiv \sum_{l} P_l e^{i\omega_l \tau}. \qquad [54]$$

$|P_{jk}|$ is the magnitude of the sum of complex numbers with fixed real lengths P_l and varying phases $\phi_l = \omega_l \tau$. In general, the single-quantum frequencies ω_l are unequal, so as τ varies these components fan out in the complex plane like different hands on a clock. The τ-averaged probability density associated with a given component is simply

$$p_l(r) = \delta(r - P_l). \qquad [55]$$

For a fixed value of τ, P_{jk} can be thought of as a complex plane random walk of q steps, where q is the number of components. The τ-averaged probability density of P_{jk} is difficult to compute exactly, but can be approximated using the central limit theorem as a two-dimensional Gaussian:

$$p(r) = \frac{1}{\pi\alpha^2} e^{-r^2/\alpha^2}. \qquad [56]$$

With this approximation,

$$\langle |P_{jk}|^2 \rangle_\tau = \overline{r^2} = \int_0^\infty \int_0^{2\pi} r^2 p(r) r dr d\phi = \alpha^2, \qquad [57a]$$

$$\langle |P_{jk}| \rangle_\tau = \bar{r} = \int_0^\infty \int_0^{2\pi} r p(r) r dr d\phi = \frac{1}{2}\sqrt{\pi}\alpha, \qquad [57b]$$

$$\xi = \frac{\overline{r^2}}{(\bar{r})^2} = \frac{4}{\pi} \approx 1.27. \qquad [57c]$$

Thus for a given line, the average over τ of the transition intensity for $t_2 = \tau$ should be 1.27 times the average intensity when τ and t_2 are varied separately.

The averaging is somewhat different for $|k\rangle$ to $|\bar{k}\rangle$ transitions. It was shown previously that $P_{k\bar{k}}$ is always purely imaginary. For such transitions, $B_{ba} = -B_{ab}$, and

$$P_{k\bar{k}} = 2i \sum_{a<b} B_{ab} \sin \omega_{ba}\tau \equiv i \sum_{l} c_l \sin \omega_l \tau. \qquad [58]$$

Each component of $P_{k\bar{k}}$ now oscillates only along the complex axis with a τ-averaged probability density given by (*43*)

$$p_l(y) = \frac{1}{\pi}[c_l^2 - y^2]^{-1/2} \qquad (y^2 \leqslant c_l^2). \qquad [59]$$

For a fixed value of τ, $P_{k\bar{k}}$ can be thought of as a one-dimensional random walk; averaged over τ its probability density will again be assumed to be a Gaussian:

$$p(y) = (2\pi)^{-1/2}\sigma^{-1}e^{-y^2/2\sigma^2}. \qquad [60]$$

In this case,

$$\xi = \frac{\langle |p_{k\bar{k}}|^2 \rangle_\tau}{\langle |p_{k\bar{k}}| \rangle_\tau^2} = \frac{\overline{y^2}}{(|\bar{y}|)^2} = \frac{\sigma^2}{(\sqrt{2/\pi}\,\sigma)^2}$$

$$= \frac{\pi}{2} \approx 1.57. \qquad [61]$$

Because spin-inversion transitions are at most a small percentage of the total number of transitions, they do not contribute much to the total magnitude spectrum intensity. Thus, as stated earlier, this total intensity at $t_2 = \tau$ should be about 1.27 times larger than the intensity when $t_2 \neq \tau$.

The ratio ξ was calculated for the totally symmetric A_1 transitions of oriented acetaldehyde by averaging over 200,000 values of τ; results are listed in Table 5. For this molecule, the four-quantum line is the only A_1 spin-inversion transition and ξ for it is 1.585. The average value of ξ for all other transitions is 1.271. Both numbers are very close to the random-walk values.

TABLE 5

ξ as a Function of Multiple-Quantum Order (A_1 Transitions)

ΔM	Benzene	Acetaldehyde
0	1.290	1.298
1	1.218	1.256
2	1.223	1.277
3	1.225	1.283
4	1.253	1.585
5	1.239	
6	1.441	

Also in Table 5 are similar results for the A_1 transitions of oriented benzene, obtained by averaging over 20,000 τ values. The average ratio for odd-quantum orders (for which there can be no spin-inversion transitions) is 1.22, not far from the predicted ratio for two-dimensional random walks. The ratio for the spin-inversion six-quantum line is 1.44. Though smaller than the prediction of the simple 1-D random walk model, this value is at least closer to $\pi/2$ than $4/\pi$.

Actually, the value of ξ relates back to the value of d, the ratio of the average dipolar coupling to the rms coupling. For systems with $d \approx 0$, the B_{ab} elements which comprise $P_{k\bar{k}}$ and which constitute the step lengths of the random walk are

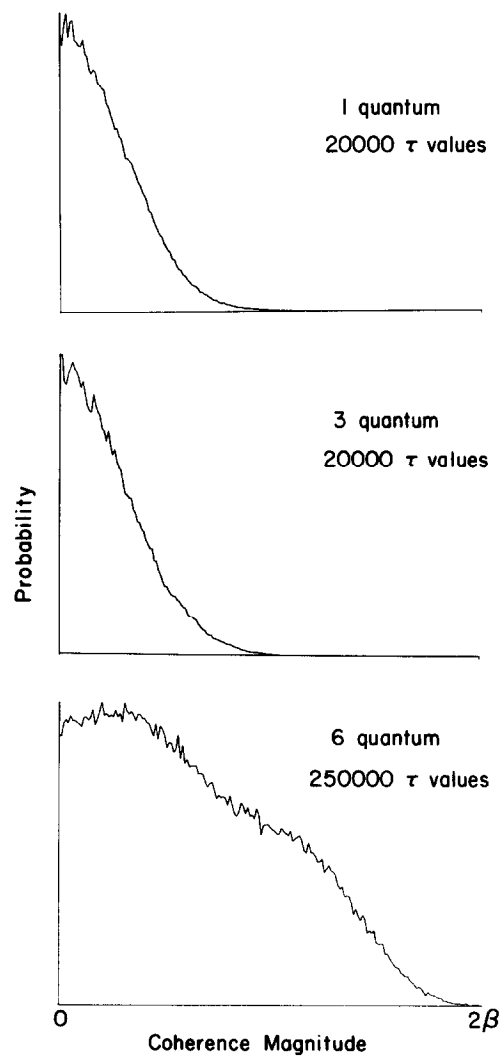

FIG. 13. Probability distribution for the average prepared coherence magnitude of A_1 transitions in oriented benzene, obtained by averaging over many values of τ. Ideally, the top two curves are profiles of two-dimensional Gaussians; the third is ideally half of a one-dimensional Gaussian.

roughly comparable in size. The central limit theorem with its prediction of a Gaussian probability density should be especially accurate and ξ should be close to $\pi/2$. In contrast, when $d \approx 1$, a few B_{ab} elements are far larger than the rest, generating a few "giant strides" in the random walk. The central limit assumption is thus less valid, and ξ is expected to lie between $\pi/2$ and its value for the single-component probability density of Eq. [59], namely $\pi^2/8 \approx 1.234$. For benzene, d is 0.776 and $\xi = 1.44$ as noted above.

In addition to the calculation of ξ values, the actual distribution of $|P_{jk}|$ for each multiple-quantum order was computed for both the benzene A_1 transitions and acetaldehyde A_1 transitions by again averaging over many values of τ. In Fig. 13 $p(r)$ vs r is plotted for benzene with $\Delta M = 1$, $\Delta M = 3$, and $\Delta M = 6$. Figure 14 displays $p(r)$ vs r for acetaldehyde. In each case except the benzene six-quantum transition, the distribution indeed appears Gaussian.

To summarize, it can be seen that choosing t_2 equal to τ is advantageous but not crucial in the three-pulse multiple-quantum experiment. When magnet homogeneity is good, one may, for optimal signal-to-noise, sample the magnetization at many values of t_2. One can then average together the magnitude MQ spectra associated with each value of t_2 (*36*), or take the two-dimensional transform (*3*, *4*) and compress the resulting magnitude spectrum along the multiple-quantum axis. When magnet homogeneity is bad, however, echoing pulses (*44*, *45*) must be added to the pulse sequence at $\tau/2$ and during the detection period. Under these circumstances

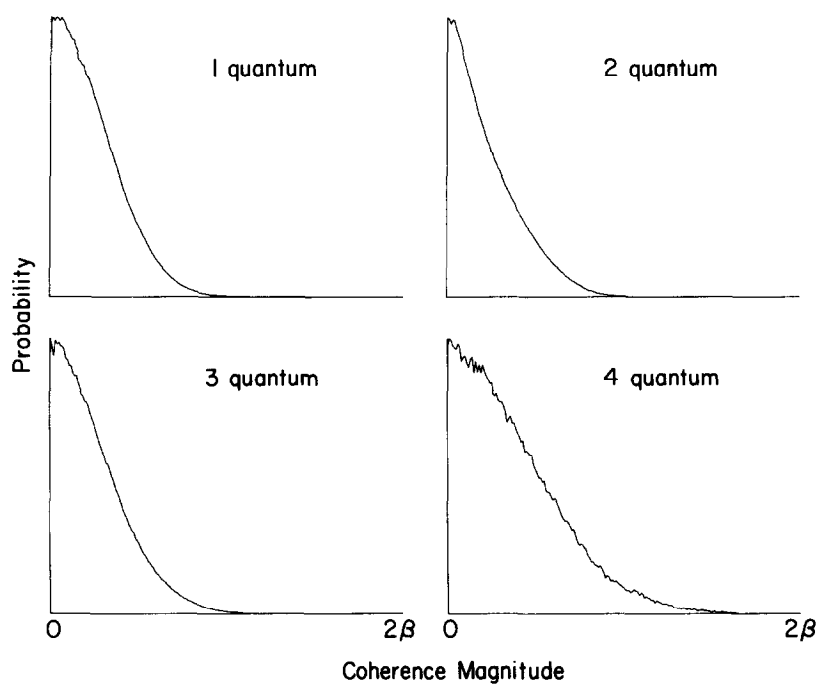

FIG. 14. Probability distribution for the average prepared coherence magnitude of A_1 transitions in oriented acetaldehyde. The coupling constants used in the calculation are those in Ref. (*24*).

(or when data storage capacity is insufficient for a 2-D experiment), the magnetization can be measured at only a limited number of points in the detection period, and one might as well choose $t_2 = \tau$ as one of them.

CONCLUSIONS

In an analysis of the basic multiple-quantum experiment, we have calculated average coherence magnitudes as a function of preparation time τ and found that in general the growth of k-quantum coherence in an anisotropic system is proportional to τ^{k-1}. Ultimate τ average intensities were then introduced as an efficient way of generating τ-independent MQ spectra. High-quantum transitions were found to be more intense than a simple statistical model would suggest, an encouraging result for future experimental work. This enhancement is most pronounced when the average dipolar coupling constant is comparable to the rms value. Finally, the $\sim$25% bulge in total spectral intensity when $t_2 = \tau$ was explained in terms of a random walk model.

ACKNOWLEDGMENTS

We thank Steven Sinton, Gary Drobny, and everyone else in the Alex Pines Multiple Quantum Task Force for useful and entertaining discussions, and Dione Carmichael for careful preparation of this manuscript. Calculations were performed on a VAX 11/780 computer system for which we are indebted to Dr. Melvin Klein and Dr. Ken Wiley of the Laboratory for Chemical Biodynamics at Lawrence Berkeley Laboratory for their cooperation and assistance. W.S.W. held a National Science Foundation Graduate Fellowship. This work was supported by the Director, Office of Energy Research, Office of Basic Energy Sciences, Materials Sciences Division of the U.S. Department of Energy under Contract DE-AC03-76SF00098.

REFERENCES

1. H. HATANAKA, T. TERAO, AND T. HASHI, *J. Phys. Soc. Jpn.* **39,** 835 (1975); H. HATANAKA AND T. HASHI, *J. Phys. Soc. Jpn.* **39,** 1139 (1975).
2. S. VEGA, T. W. SHATTUCK, AND A. PINES, *Phys. Rev. Lett.* **37,** 43 (1976); S. VEGA AND A. PINES, *J. Chem. Phys.* **66,** 5624 (1977).
3. W. P. AUE, E. BARTHOLDI, AND R. R. ERNST, *J. Chem. Phys.* **64,** 2229 (1976).
4. A. WOKAUN AND R. R. ERNST, *Chem. Phys. Lett.* **52,** 407 (1977).
5. A. PINES, D. WEMMER, J. TANG, AND S. SINTON, *Bull. Am. Phys. Soc.* **23,** 21 (1978).
6. G. DROBNY, A. PINES, S. SINTON, D. P. WEITEKAMP, AND D. WEMMER, *Faraday Symp. Chem. Soc.* **13,** 49 (1979).
7. G. BODENHAUSEN, *Prog. NMR Spectrosc.* **14,** 137 (1981).
8. D. P. WEITEKAMP, *Adv. Magn. Reson.* **11,** 111 (1983).
9. S. HSI, H. ZIMMERMANN, AND Z. LUZ, *J. Chem. Phys.* **69,** 4126 (1978).
10. J. TANG AND A. PINES, *J. Chem. Phys.* **73,** 2512 (1980).
11. S. SINTON AND A. PINES, *Chem. Phys. Lett.* **76,** 263 (1980).
12. A. BAX, R. FREEMAN, AND S. P. KEMPSELL, *J. Am. Chem. Soc.* **102,** 4849 (1980); A. BAX, R. FREEMAN, AND T. A. FRENKIEL, *J. Am. Chem. Soc.* **103,** 2102 (1981).
13. A. WOKAUN AND R. R. ERNST, *Mol. Phys.* **36,** 317 (1978).
14. M. E. STOLL, A. J. VEGA, AND R. W. VAUGHAN, *J. Chem. Phys.* **67,** 2029 (1977).
15. R. POUPKO, R. L. VOLD, AND R. R. VOLD, *J. Magn. Reson.* **34,** 67 (1979).
16. G. BODENHAUSEN, R. L. VOLD, AND R. R. VOLD, *J. Magn. Reson.* **37,** 93 (1980).
17. J. TANG AND A. PINES, *J. Chem. Phys.* **72,** 3290 (1980).
18. S. EMID, A. BAX, J. KONIJNENDIJK, J. SMIDT, AND A. PINES, *Physica B* **96,** 333 (1979).

19. D. WEMMER, Ph.D. Thesis, University of California, Berkeley, 1979 (published as Lawrence Berkeley Laboratory Report LBL-8042).
20. A. ALLOUCHE, F. MARINELLI, AND G. POUZARD, *J. Magn. Reson.* **53,** 65 (1983).
21. G. BODENHAUSEN AND C. M. DOBSON, *J. Magn. Reson.* **44,** 212 (1981).
22. P. J. HORE, E. R. P. ZUIDERWEG, K. NICOLAY, K. DIJKSTRA, AND R. KAPTEIN, *J. Am. Chem. Soc.* **104,** 4286 (1982); P. J. HORE, R. M. SCHEEK, AND R. KAPTEIN, *J. Magn. Reson.* **52,** 339 (1983).
23. L. BRAUNSCHWEILER, G. BODENHAUSEN, AND R. R. ERNST, *Mol. Phys.* **48,** 535 (1983).
24. D. P. WEITEKAMP, J. R. GARBOW, J. B. MURDOCH, AND A. PINES, *J. Am. Chem. Soc.* **103,** 3578 (1981); J. R. GARBOW, D. P. WEITEKAMP, AND A. PINES, *J. Chem. Phys.* **79,** 5301 (1983).
25. A. A. BOTHNER-BY AND S. M. CASTELLANO, "Computer Programs for Chemistry" (D. F. Detar, Ed.), Vol. 1, Benjamin, New York, 1968.
26. S. W. SINTON, Ph.D. Thesis, University of California, Berkeley, 1981 (published as Lawrence Berkeley Laboratory Report LBL-13604).
27. W. S. WARREN, J. B. MURDOCH, AND A. PINES, *J. Magn. Reson.* **60,** 236 (1984).
28. J. W. EMSLEY AND J. C. LINDON, "NMR Spectroscopy Using Liquid Crystal Solvents," Pergamon, Oxford, 1975.
29. A. A. MAUDSLEY, A. WOKAUN, AND R. R. ERNST, *Chem. Phys. Lett.* **55,** 9 (1978).
30. A. SAUPE, *Z. Naturforsch. A* **20,** 572 (1965).
31. W. K. RHIM, A. PINES, AND J. S. WAUGH, *Phys. Rev. B* **3,** 684 (1971).
32. Y. S. YEN AND A. PINES, *J. Chem. Phys.* **78,** 3579 (1983).
33. D. P. WEITEKAMP, J. R. GARBOW, AND A. PINES, *J. Magn. Reson.* **46,** 529 (1982).
34. D. JAFFE, R. R. VOLD, AND R. L. VOLD, *J. Magn. Reson.* **46,** 475 (1982).
35. A. G. AVENT, *J. Magn. Reson.* **53,** 513 (1983).
36. W. S. WARREN, Ph.D. Thesis, University of California, Berkeley, 1980 (published as Lawrence Berkeley Laboratory Report LBL-11885).
37. C. S. YANNONI, *J. Am. Chem. Soc.* **92,** 5237 (1970).
38. H. S. GUTOWSKY, D. W. MCCALL, AND C. P. SLICHTER, *J. Chem. Phys.* **21,** 279 (1953).
39. P. L. CORIO, "Structure of High-Resolution NMR Spectra," Chap. 4, Academic, New York, 1966.
40. J. B. MURDOCH, Ph.D. Thesis, University of California, Berkeley, 1982 (published as Lawrence Berkeley Laboratory Report LBL-15254).
41. W. S. WARREN AND A. PINES, *J. Chem. Phys.* **74,** 2808 (1981).
42. A. D. BAIN AND S. BROWNSTEIN, *J. Magn. Reson.* **47,** 409 (1982).
43. F. REIF, "Fundamentals of Statistical and Thermal Physics," p. 31, McGraw-Hill, New York, 1965.
44. E. L. HAHN, *Phys. Rev.* **80,** 580 (1950).
45. H. Y. CARR AND E. M. PURCELL, *Phys. Rev.* **94,** 630 (1954).